Breeding and preliminarily phenotyping of a congenic mouse model with alopecia areata

Mei-Er GU, Xiao-Ming SONG, Chun-Feng ZHU，Hong-Ping YIN, Gui-Jie LIU, Li-Ping YU, Wei-Wei YANG, Li-Feng NI, Yan-Li ZHANG, Bao-Jin WU*

Laboratory of Experimental Animal Science, *Hangzhou Normal University*, *Hangzhou* 310036, *China*

Abstract: In the current study, the alopecia areata gene was introduced into the C57BL/6 (B6) mouse through repeated backcrossing/intercrossing, and the allelic homozygosity of congenic AA^{tj}mice (named B6.KM-*AA*) was verified using microsatellites. The gross appearance, growth characteristics, pathological changes in skin, and major organs of B6.KM-*AA* mice were observed. Counts and proportions of $CD4^+$ and $CD8^+$ T lymphocytes in peripheral blood were determined by flow cytometry. Results show that congenic B6.KM-*AA* mice were obtained after 10 generations of backcrossing/intercrossing. B6.KM-*AA* mice grew slower than B6 control mice and AA skin lesions were developed by four weeks of age. The number of hair follicles was reduced, but hair structures were normal. Loss of hair during disease progression was associated with $CD4^+$ and $CD8^+$ T lymphocytes infiltration peri- and intra-hair follicles. No pathological changes were found in other organs except for the skin. In the peripheral blood of B6.KM-*AA* mice, the percentage of $CD4^+$ T cells was lower and percentage of $CD8^+$ T cells higher than in control mice. These findings indicate that B6.KM-*AA* mice are characterized by a dysfunctional immune system, retarded development and T-cell infiltration mediated hair loss, making them a promising new animal model for human alopecia areata.

Keywords: Alopecia areata; Congenic mouse; T-lymphocytes; CD4; CD8

Alopecia areata (AA) is a common disease in humans, can affect any hair-bearing region of the body, and usually shows with acute non-inflammatory alopecia parvimaculata, but unfortunately its underlying mechanisms are not fully understood but it is correlated with genetic background, emotional stress, endocrine dyscrasia and autoimmunity. Hereditary susceptibility is one of the most important factors of AA, and approximately 25% patients have affected family members. Due to increasing stress from study and work, a growing number of people are affected by hair loss. In some cases, it results in psychological effects such as reduced self-esteem, and in extreme cases may even induce depression or suicide. It is therefore vital to investigate the underlying mechanisms of AA, identify the related genes and explore possible therapeutic targets (Sun et al, 2008).

AA mouse models have played important roles in AA studies. For example, Sundberg et al (1994) found that 20% of C3H/HeJ mice spontaneously develop adult onset AA by 18 months of age, and the progression of this complicated multi-genetic disorder is quite similar to the clinical symptoms of human AA. In addition to laboratory mice, AA-like hair loss has been noticed in inbred Dundee rats (McElwee et al, 1996). Recently, with availabilities of C3H/HeJ mice and Dundee rats, concerted attempts have been made to understand the genetics, pathogenesis and treatment of AA (Michie et al, 1991; McElwee et al, 2002; Sundberg et al, 1996); however, due to the low incidence (20%) of AA in C3H/HeJ mice, validation of a new AA animal model is necessary.

The mice used here (current name: Alopecia Areata Tongji, AA^{tj}) are characterized by progressive hair loss

Received: 25 November 2013; Accepted: 25 December 2013
Foundation items: This work was supported by the Public Program of the Science Technology Department, Zhejiang (2011C37077) and the National Natural Science Foundation of China (31071092).
* Corresponding author, E-mail: baojinwu@163.com

and were initially discovered 10 years ago during the propagation of KM mice by the Laboratory Animal Center at Tongji University. During years of conservation breeding, attempts have previously been made to introduce the mutant genes into other inbred strains by repeated backcrossing/intercrossing, but the documntation related to this process are missing. To establish an inbred mice strain with a purified genetic background, we introduced the *AA* gene into C57BL/6 (B6) mice by repeated backcrossing/intercrossing. The development and pathogenesis of this congenic inbred AA mouse strain (B6.KM-*AA*) was then evaluated. The validation of this B6.KM-*AA* mice model will likely facilitate future AA mutant gene location, identification and related investigations into the biological characteristics of this condition.

MATERIALS AND METHODS

Experimental animals

AA^{tj} mice were acquired from Hangzhong Normal University four years ago. Clean AA^{tj} mice and control B6 mice were provided by the Laboratory of Experimental Animal Science, Hangzhong Normal University (Laboratory Animal Production and Use License: SCXK [Zhejiang] 2011-0048; SYXK [Zhejiang] 2011-0157). Experimental animals were housed in protective animal rooms with a 12/12 h light cycle, with temperature at 23±2 °C and humidity at 55±5%. Animals were fed Co60 irradiated food *ad libitum*. Caging and bedding materials were changed frequently and sterilized using heat.

Experimental equipment and reagents

Reagents used in polymerase chain reaction (PCR) were from Sangon Biotech (Shanghai, China). Monoclonal antibodies ($CD4^+$ (ab25475), $CD8^+$ (ab25478)) and Rat IgG (horse radish peroxidase) (ab6734) were products of Abcam (Cambridge, UK). CD3-PE/Cy7, CD4-PE, CD8-FITC and parallel control antibodies were from BD Bioscience (San Diego, CA). Experimental equipment and manufacturers were: PCR machine (BIOS, 1000), electrophoresis apparatus (Tanon, EPS300), gel imaging system (Tomon, 2500), paraffin embedding machine (MicRom, AP280), rotary microtome (MicRom, HM3-35E), pathological tissue floating and drying apparatus (Huali Electronics, Changzhou, China), flow cytometry (BD, FACSCalibur, Becton Dickinson, San Jose, CA, USA)), and upright camera microscope (Olympus, BX51).

Breeding of congenic B6.KM-*AA* mice

F1 *AA* mutant gene carriers without the AA phenotype were hybrids of AA phenotype mice and B6 mice. F2 mice with either the AA or normal phenotype were bred through F1 mice intercrossing. F3 mice were obtained by backcrossing AA phenotype F2 with B6 mice. Then, F4 mice were bred through F3 mice intercrossing. After several generations of repeated intercrossing, AA phenotype F10 mice were established for strain conservation.

Homozygosity evaluation of congenic B6.KM-*AA* mice

Genomic DNA extraction from the tip of the tails (0.5 cm) of F10 congenic B6.KM-*AA* mice was purified by protease K digestion followed by phenol: chloroform extraction. Thirty-nine mouse microsatellites established by our laboratory (Wu et al, 2003) were applied in the homozygosity evaluation.

Recessive inheritance validation

During breeding, total numbers of the AA phenotype and normal F2, F4, F6, F8, F10 mice were calculated. The practical ratio of mutant mice to normal mice and theoretical ratio derived from recessive inheritance were compared. Then, the practical number and percentage of AA phenotype G3 mice were compared with theoretical values derived from recessive inheritance. G3 mice were bred through the backcrossing of G2 (hybrids of B6.KM-*AA* mice and B6 mice) and G1 mice (B6.KM-AA mice).

Developments of congenic B6.KM-*AA* mice

Hair growth in litters from birth to 12 weeks of age was observed, and animal weight from birth to 8 weeks of age was recorded. Three-week-old males and females were caged separately and gains in mass were recorded and statistical analysis was done by taking normal B6 mice bred by our animal center as controls.

Hair observation of congenic B6.KM-*AA* mice

Hair samples from dorsal areas of the should blades of six 8-week-old B6.KM-*AA* mice (3 males, 3 females) and six B6 mice (3 males, 3 females) were mounted on dimethyl benzene marinated glass slides, sealed with neutral balsam and then observed under a microscope.

Major organs and pathology of skin tissues of B6.KM-*AA* mice

Mice used in the hair observation were euthanatized by cervical dislocation. Major organs, including brain, heart, liver, spleen, lung, kidney, thymus, adrenal gland,

testicle, appendix testis, uterus and ovary were fixed by 10% formalin. After dehydration, infiltration, embedding, sectioning and Hematoxylin-Eosin (HE) staining they were observed under a light scope.

Three males and 3 females of B6.KM-*AA* mice and B6 mice by birth, 2 weeks, 4 weeks, 6 weeks, 8 weeks and 12 weeks of age were euthanatized by cervical dislocation. Dorsal skin samples were fixed using 10% formalin. After dehydration, infiltration, embedding, sectioning and HE staining skin tissue pathology was observed under a light scope.

Immunohistochemistry staining

Paraffin sections of skin tissues were used in horseradish peroxidase conjugated $CD4^+$ and $CD8^+$ immunohistochemical experiment. Working concentrations of $CD4^+$, $CD8^+$ and rat IgG (HRP) were 1:50, 1:50 and 1:100, respectively. Sections were incubated in primary antibody at 4 °C overnight, and then in secondary antibody at 37 °C for 60 min, followed with chromogenic staining by 3, 3'-diaminobenzidine (DAB) and Hematoxylin counterstaining. Phosphate Buffered Saline (PBS) was used as the negative control of primary antibody.

Analysis of peripheral blood $CD4^+$ and $CD8^+$ T lymphocytes

Retro-orbital venous blood samples (200 μL) were collected from three male and three female B6. KM-*AA* mice and B6 mice at 8 weeks of age, and then transferred into anticoagulant sodium heparin tubes. Tubes were gently converted to prevent coagulating and were kept on ice. Next, 100 μL blood samples were transferred into polystyrene tubes with CD3-PE/Cy7 (5 μL), CD4-PE (5 μL) and CD8-FITC (2 μL) monoclonal antibodies. Meanwhile, negative and blank controls were set. Blood samples were incubated in the dark at 4 °C for 30 min and then 2 mL 1× FACS lysing solution was added. After incubation in the dark at 4 °C for 15 min, samples were centrifuged at 4 °C for 5 min at 1500 r/min. Supernatants were discarded and cell pellets were rinsed with ice-cold PBS 1−2 times, then centrifuged again at 4 °C for 5 min at 1 500 r/min. Supernatants were discarded and cell pellets were resuspended with 400 μL PBS. Five thousand cells/tube went through flow cytometry and numbers of $CD3^+$, $CD4^+$ and $CD8^+$ cells were recorded. Results were analyzed using Cell Quest.

Statistical analysis

All statistical analysis was conducted via SPSS17.0 (SPSS Inc, Chicago, IL). Heritability patterns were determined using *chi*-square tests. All other data were analyzed using independent-sample *t*-tests. All results are expressed as mean±*SD*.

RESULTS

Breeding of congenic B6.KM-*AA* mice

AA^{tj} mice came from white KM mice and were characterized by black hair and a close appearance to B6 mice. After two years and 10 generations of backcrossing/intercrossing with B6 mice, we obtained F10 AA mice. This AA mutant mice strain was then conserved by inbred breeding and named B6.KM-*AA* according to naming regulations of gene introgession. After 10 generations of crossing, theoretically, the genetic background of B6.KM-*AA* mice is 96.88% $[1-(50\%)^5]$, consistent with that of B6 mice. Moreover, homozygosity detection based on 19 microsatellites (D1Mit416, D1Mit180, D2Mit62, D2Mit249, D4Mit214, D4Mit55, D5Mit356, D5Mit409, D7Mit230, D7Mit318, D7Mit203, D10Mit70, D11Mit229, D15Mit171, D15Mit29, D17Mit123, D17Mit224, D18Mit187 and D18Mit149) showed a single band for each locus of all mice, indicating the B6 genetic background of this congenic B6.KM-*AA* mice strain (Figure 1).

B6.KM-*AA* recessive inheritance confirmation

During the breeding of B6.KM-*AA* mice, among the 235 individuals obtained from F2, F4, F6, F8 and F10

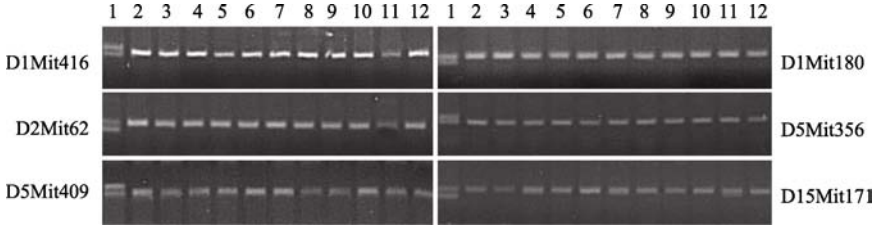

Figure 1 Homozygosity detection of microsatellite loci

Lane 1: B6D2F1 control; Lane 2−12: B6.KM-*AA* mice.

generations, 49 were with AA phenotype and 186 were normal. *Chi*-square values and *P* values were calculated by comparing mice numbers with recessive inheritance patterns of a single gene (χ^2=0.753, *P*=0.385). Therefore, the single recessive inheritance of the *AA* mutant gene was confirmed. The G2 hybrids of B6. KM-*AA* and B6 mice were all normal, whereas, 24 AA phenotype mice were bred among 54 hybrids of G2 and B6.KM-*AA* mice. The single recessive inheritance of B6.KM-*AA* mice was also confirmed (χ^2=0.12, *P*=0.729).

Development observation of B6.KM-*AA* mice

Hair growth in juvenile B6.KM-*AA* mice was normal. Patchy hair loss was developed by 4 weeks of age on the head and face. Symptoms were more obvious with increasing age and were severe by 12 weeks of age, characterized by sparse, short and thin hair (Figure 2). However, hair structures were normal with aligned internal medulla (not shown in the figure). From birth to 4-weeks-old, B6.KM-*AA* mice were lighter than control B6 mice. No significant difference in mass between 5-week-old B6.KM-*AA* males and controls was observed, whereas, female B6.KM-*AA* mice were consistently and significantly lighter than controls until puberty. These patterns indicate retarded development in B6.KM-*AA* mice compared with B6 mice (Figure 3).

Figure 2 Hair growth in B6.KM-*AA* mice at different developmental stages

A, B, C, D, E, F and G: Developmental stages of birth, 1-week-, 2-week-, 4-week-, 6-week-, 8-week- and 12-week-old, respectively.

Major organs, pathology and immunology of skin tissues

From birth to 2 weeks of age, no differences in skin tissue between B6.KM-*AA* and B6 mice were found. Lymphocyte infiltration could be seen around hair follicles

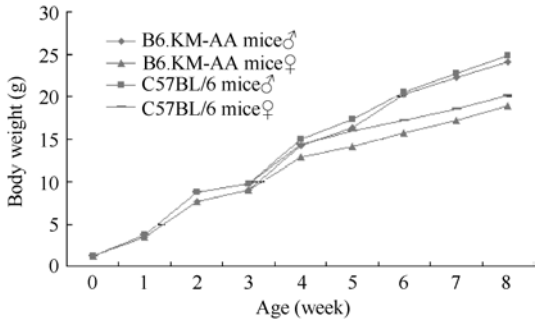

Figure 3 Body weight gain curvature of congenic B6.KM-*AA* mice and B6 mice

in B6.KM-*AA* mice by 4 weeks of age and worsened with disease progression. Lymphocyte infiltration in hair follicles was obvious, accompanied with hair follicle dystrophy and number reduction. Those symptoms were most severe in 12-week-old B6.KM-*AA* mice and could not be seen in control B6 mice. Monoclonal immunohistochemistry showed $CD8^+$ T lymphocyte positive expression around hair follicles and the root sheath derived from skins of B6.KM-*AA* mice, whereas, only small $CD4^+$ T lymphocytes expression was found around hair follicles (Figure 4)

No significant abnormality was found in paraffin sections of major organs of B6.KM-*AA* mice, including brain, heart, liver, spleen, lung, kidney, thymus, adrenal gland and intestine (not shown).

Analysis of $CD4^+$ and $CD8^+$ T lymphocytes in peripheral blood of B6.KM-*AA*

No significant differences in peripheral blood total lymphocytes between B6.KM-*AA* mice and normal control B6 mice were found. Compared with normal control B6 mice, B6.KM-*AA* mice had higher expression of $CD8^+$ T lymphocytes, but lower expression of $CD4^+$ T lymphocytes (Figure 5, Table 1).

Table 1 Peripheral blood $CD4^+$ and $CD8^+$ T lymphocytes of B6.KM-*AA* mice

	B6.KM-*AA* mice (mean±*SD*)	B6 mice (mean±*SD*)	*P* value (*t*-test)
CD3 (%)	57.24±5.23	55.80±4.62	0.626–0.617
CD4 (%)	30.35±4.47	36.42±4.43	0.036–0.041
CD8 (%)	26.89±3.16	19.39±0.59	<0.01

DISCUSSION

Although AA^{tj} mice were first identified and isolated over 10 years ago, research progression has been inconsistent

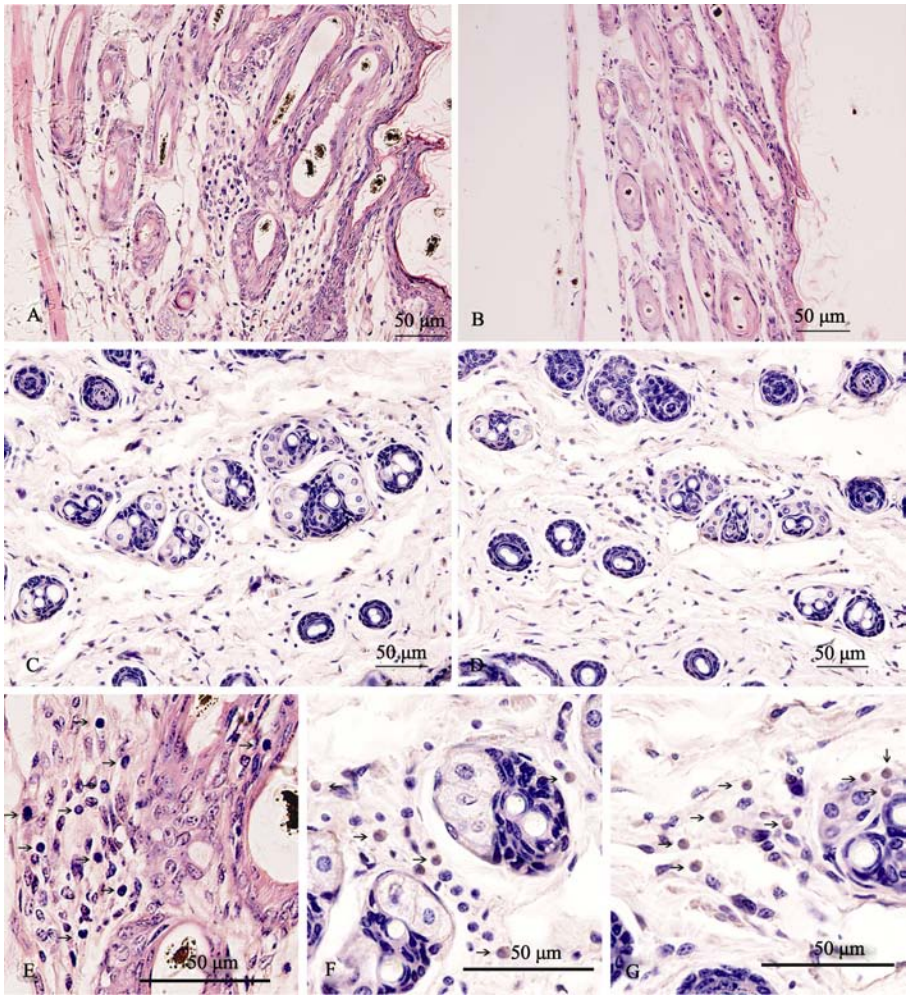

Figure 4 Lymphocyte infiltrations in hair follicles of B6.KM-*AA* mice

A, E: Dorsal skin of 8-week-old B6.KM-*AA* mice, HE staining, lymphocyte infiltrations could be seen peri- and intra- hair follicles; B: Dorsal skin of 8-week-old B6 mice, HE staining, no lymphocytes infiltrations could be seen around hair follicles; C, F: $CD4^+$ immunohistochemistry staining of the dorsal skin of 8-week-old B6.KM-*AA* mice, yellow-brown positive $CD4^+$ T-lymphocytes could be seen around hair follicles; D, G: $CD8^+$ immunohistochemistry staining of the dorsal skin of 8-week-old B6.KM-*AA* mice, yellow-brown positive $CD8^+$ T-lymphocytes could be seen around and inside of hair follicles.

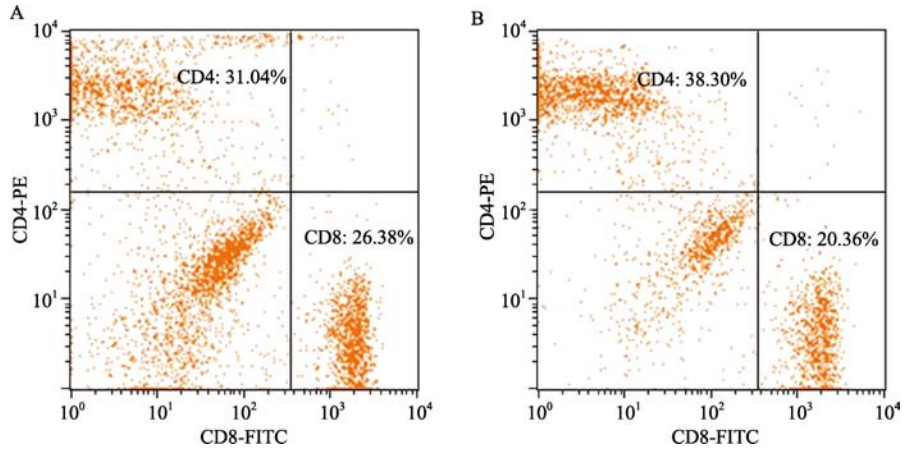

Figure 5 Two dimensional lattice chart of peripheral blood $CD4^+$ and $CD8^+$ T lymphocytes

A: B6.KM-*AA* mice; B: B6 mice.

and not well documented. AA^{tj} mice were originally from white KM mice, but until now, their black hair and body appearance were quite close to B6 mice. The uncertainty in genetic background has hindered studies and the

efficacy of this mouse model. The most important component of our study is the successful introduction of the *AA* mutant gene into a B6 background. After 10 generations of continuous introduction over two years, theoretically, the genetic background consistency of B6.KM-*AA* with B6 has reached 96.88% ($1-(50\%)^5$). In general, an inbred strain needs 20 generations of intercrossing and the allele homozygosity should reach 98.6%. In our case, taking into account B6-like characteristics AA^{tj} mice originally had, we assume the allele homozygosity of B6.KM-*AA* is over 96.88% and is relatively stable. Allele homozygosity detection conducted with microsatellite markers indicates the single genetic background of B6.KM-*AA* mice. More importantly, this purified genetic background does not influence the development of the AA phenotype in B6.KM-*AA* mice, but clarifies the single genetic recessive inheritance of the *AA* mutant gene, which can be used in model characteristic analysis and related genetic chromosome localization.

Symptoms of patchy hair loss initiated by 4 weeks of age in B6.KM-*AA* mice and get worse with age. Hair follicle dystrophy and reduction as well as $CD4^+$ and $CD8^+$ T lymphocyte infiltrations around hair follicles are more obvious with disease progression. Low expression of $CD4^+$ T lymphocytes, but high expression of $CD8^+$ T lymphocytes in peripheral blood of B6.KM-*AA* mice compared with normal control mice indicates immune dysfunction. It is believed that the loss of hair follicles is mediated by T lymphocyte infiltration. The mechanisms of AA are yet to be determined, but most researchers believe it is a systemic autoimmune disorder. Studies on C3H/HeJ mice claimed that the main reason for AA is because $CD4^+$ and $CD8^+$ T lymphocytes attack the body's own anagen hair follicles and suppress or stop hair growth, a process which TNF-α, IL-6, IL-12, IFN-γ, IL-10, IL-4 and many other cell factors also play a role in (McElwee et al, 1998). McElwee et al (1996) and Freyschmidt-Paul et al (2000) found that using monoclonal antibodies to reduce counts of $CD4^+$ and $CD8^+$ T lymphocytes and inhibit inflammatory cell infiltrations restrains the development of AA. Perret et al (1984) found that the percentage of $CD8^+$ T lymphocytes in peripheral blood of human AA patients was significantly low, whereas around hair follicles the ratio of $CD4^+/CD8^+$ is only 4:1. Chen et al (2005) adopted immunohistochemistry techniques to evaluate T lymphocytes in skin lesions of human AA patients and found that during the active phase and stable phase, cell infiltrations of $CD4^+$ T lymphocytes are significantly higher than $CD8^+$ T lymphocytes around hair follicles and vessels. Huang et al (2007) reported that in both minor and severe cases of AA, expressions of $CD4^+$ and $CD8^+$ T lymphocytes are all higher than those of control groups. Our results presented here support the idea that AA is related to cellular immunity and T lymphocyte infiltration in hair follicles plays an important role in disease progression. However, further questions such as the disorder in $CD4^+/CD8^+$ lymphocytes remain unanswered.

Over 14 mice strains have been reported with sparse hair phenotype (Wu et al, 2009; Zang et al, 2009; Li et al, 199; Tian et al, 2004), but experience congenital hair loss like in the $snthr^{-1Bao}$ mice strain bred in our lab. Therefore, their hair loss symptoms are neither required nor progressive as in human AA (Wu et al, 2010; Wu et al, 2009). C3H/HeJ mice are a widely applied AA animal model. Sundberg et al (2003) identified the pathogenic QTL locus on the 17th chromosome of C3H/HeJ mice, but relevant functional research is difficult. C3H/HeJ mice have also been used in medication research and development. It has been reported that SADBE (squaric acid dibutylester), DPCP (diphenylcyclopropenone), glucocorticosteroid, cyclosporine (CsA), tacrolimus (FK506) and minoxidil all promote hair regeneration (Sun et al, 2008). However, although the pathology in C3H/HeJ mice is similar to that in humans, the low incidence (20%) and uncertainty in identifying pathogenic genes have hampered its application as a human AA mouse model. Moreover, the homologies of pathogenic AA genes between humans and mice are pivotal in the establishment of an animal model (Mao & Zheng, 2006; Peters et al, 2007). The *AA* mutant gene in our study is a spontaneous mutation and characterized by single genetic recessive inheritance. Disease progression is close to that in human AA patients, which is beneficial for future pathogenic gene localization and colonial identification. In summary, the B6.KM-*AA* mice bred in our study are a promising AA animal model, and can be used in studies into the molecular mechanisms of AA, observations of medication efficacy and strain conservation of economic fur animals.

References

Chen LF, Shi WP, Liu JH, Chen XM, Qin XW, Hao SY, Zheng XG, Shang YL, Wang YF. 2005. A study on infiltrating T-lymphocytic phenotype and Fas expression in skin lesion area of pelade patients. *Shanxi Medical Journal,* **34**(1): 9-11. (in Chinese)

Freyschmidt-Paul P, Seiter S, Zöller M, König A, Ziegler A, Sundberg JP, Happle R, Hoffmann R. 2000. Treatment with an anti-CD44v10-specific antibody inhibits the onset of alopecia areata in C3H/HeJ mice. *Journal of Investigative Dermatology,* 115(4): 653-657.

Huang WN, Hou XZ, Lu HQ, Lu HM, Xu X. 2007. Studies on the relationship between T lymphocyte subtypes and alopecia areata. *Southern China Journal of Dermato-Venereology,* **14**(4): 208-210. (in Chinese)

Li SR, Wang DP, Lan H, Zang WY, Ge BS, Li JQ, Wang CE, Lu YF, Lu YY, Li RF. 1999. A new mouse mutant gene mapping. *Chinese Science Bulletin,* **44**(7): 50-55. (in Chinese)

Mao L, Zheng WJ. 2006. Combining comparative genomics with de novo motif discovery to identify human transcription factor DNA-binding motifs. *BMC Bioinformatics,* **7**(Suppl 4): S21.

McElwee KJ, Boggess D, King LE Jr, Sundberg JP. 1998. Experimental induction of alopecia areata-like hair loss in *C3H/HeJ* mice using full-thickness skin grafts. *Journal of Investigative Dermatology,* **111**(5): 797-803.

McElwee KJ, Pickett P, Oliver RF. 1996. The DEBR rat, alopecia areata and autoantibodies to the hair follicle. *British Journal of Dermatology,* **134**(1): 55-63.

Michie HJ, Jahoda CA, Oliver RF, Johnson BE. 1991. The DEBR rat: an animal model of human alopecia areata. *British Journal of Dermatology,* **125**(2): 94-100.

McElwee KJ, Hoffmann R. 2002. Alopecia areata-animal models. *Clinical and Experimental Dermatology,* **27**(5): 410-417.

McElwee KJ, Spiers EM, Oliver RF. 1996. *In vivo* depletion of $CD8^+$ T cells restores hair growth in the DEBR model for alopecia areata. *British Journal of Dermatology,* **135**(2): 211-217.

Perret C, Wiesner-Menzel L, Happle R. 1984. Immunohistochemical analysis of T-cell subsets in the peribulbar and intrabulbar infiltrates of alopeciaareata. *Acta Dermato Venereologica,* **64**(1): 26-30.

Peters LL, Robledo RF, Bult CJ, Churchill GA, Paigen BJ, Svenson KL. 2007. The mice as a model for human biology: a resource guide for complex trait analysis. *Nature Reviews Genetics,* **8**(1): 58-69.

Sundberg JP, Cordy WR, King LE Jr. 1994. Alopecia areata in aging C3H/HeJ mice. *Journal of Investigative Dermatology,* **102**(6): 847-856.

Sundberg JP, Boggess D, Silva KA, McElwee KJ, King LE, Li R, Churchill G, Cox GA. 2003. Major locus on mouse chromosome 17 and minor locus on chromosome 9 are linked with alopecia areata in C3H/HeJ mice. *Journal of Investigative Dermatology,* **120**(5): 771-775.

Sundberg JP, King LE Jr. 1996. Mouse mutations as animal models and biomedical tools for dermatological research. *Journal of Investigative Dermatology,* **106**(2): 368-376.

Sun J, Silva1 KA, McElwee KJ, King LE Jr, Sundberg JP. 2008. The C3H/HeJ mouse and DEBR rat models for alopecia areata: review of preclinical drug screening approaches and results. *Experimental Dermatology,* **17**(10): 793-805.

Tian M, Xiong YL, Wang WY, Zhang YD. 2004. Kunming rhinos in mice and its molecular genetic. *Chinese Science Bulletin,* **49**(1): 74-80. (in Chinese)

Wu BJ, Mao HH, Zhu H, Yan ZF, Yang L, Sun Q, Xu XM, Xue ZF, Li HD. 2003. PCR conditions and application of 39 mouse microsatellites. *Acta Laboratorium Animalis Scientia Sinica,* **11**(4): 216-220. (in Chinese)

Wu BJ, Mao HH, Zeng YM, Yin LJ, Yin XS, Yang WW, Kang XD, Liu GJ, Yu LP, Gu ME, Wu PL. 2009. Fine Mapping and Identifying the Mutation Gene of *snthr*-^{1Bao} Scant Hair Mouse. *Zoological Research,* **30**(3): 267-275. (in Chinese)

Wu BJ, Zeng YM, Mao HH, Yin LJ, Zhu J, Yang W W, Yin XS, Wu PL, Zhang WD. 2010. Mapping of genetic modifiers of Plcd1 in scant hair mice (*snthr*$^{-1Bao}$). *Chinese Science Bulletin,* **55**(35): 4026-4031.

Zang WQ, Yang X, Wang T, Xuan XY, Li M, Du Y. 2009. Orientation and analysis of Yuyi hairless mice hairless gene mutation point. *Journal of Zhengzhou University: Medical Sciences,* **44**(6): 1144-1145. (in Chinese)